Epitaxial growth and superconducting anisotropy of $PbSr_2Y_{1-x}Ca_xCu_2O_{7+\delta}$ thin films

S. Komori,* R. Inaba, I. Kakeya, and M. Suzuki
Department of Electronic Science and Engineering, Kyoto University, Katsura, Nishikyo-ku, Kyoto 615-8510, Japan

K. Kaneko and S. Fujita
Photonics and Electronics Science and Engineering Center, Kyoto University, Katsura, Nishikyo-ku, Kyoto 615-8520, Japan

(Dated: today)

Thin films of single-crystal $Pb_{1-y}Bi_ySr_2Y_{1-x}Ca_xCu_2O_{7+\delta}$ (PbBi1212) were grown on $SrTiO_3$ (100) substrates by a two-step growth technique in which an amorphous film is annealed at 970 °C in a closed ceramic container prepared using the same material as the film. We find that PbBi1212 exhibits superconductivity when the Ca concentration x exceeds 0.3. The resistivity measurement in a magnetic field reveals that the coherence lengths of Pb1212 ($y = 0$) are approximately 25 and 2.7 Å along the *ab*-plane and the *c*-axis, respectively. The highest onset temperature for the superconducting transition attained in the present study is 65 K.

Keywords: Pb-1212, ex-situ growth, anisotropy

arXiv:1403.8004v1 [cond-mat.supr-con] 31 Mar 2014

I. INTRODUCTION

The family of 1212 cuprates has single block layers and involves capable materials for superconducting wires because their anisotropy is less than that of the 2212 and 2223 families, which both have double block layers bonded by van der Waals forces. The crystal structure of Pb1212 is very similar to that of $TlBa_2CaCu_2O_{7+\delta}$ (Tl1212) and $HgBa_2CaCu_2O_{6+\delta}$ (Hg1212), both of which have a critical temperature T_c greater than 100 K. Pb1212 is expected to be less anisotropic than Tl1212 and Hg1212 because the ionic radius of the element account for the block layers is the smallest in the series ($r_{Hg} \approx r_{Tl} > r_{Pb}$). Among the Pb1212 compounds, $Pb_{1-y}Bi_ySr_2Y_{1-x}Ca_xCu_2O_{7+\delta}$ (PbBi1212)[1–4] and $Pb_{1-y}Cu_ySr_2Y_{1-x}Ca_xCu_2O_{7+\delta}$ (PbCu1212)[5,6] are of specific importance for industry because they mainly consist of the ubiquitous elements Pb and Ca rather than the more exotic Bi and Y, which are currently used for high-T_c superconducting wires. However, for Pb1212, the superconducting properties such as anisotropy and critical current are inadequately understood because of the difficulty of obtaining single-crystal samples of this material. This lack of reliable samples, has even led to claims that PbBi1212 is non-superconducting and the reported superconductivity of PbBi1212 ($T_c = 92$ K[2]) is attributed to the secondary phase of Bi2212. Therefore, this study aims to verify the superconductivity of PbBi1212 by growing single-crystal PbBi1212 epitaxial films.

Growing thin films of cuprates that incorporate Pb and Bi is extremely challenging because their vapor pressure is very high to maintain the chemical composition of the film at the growth temperature of approximately 700 °C. Karimoto and Naito succeeded in growing an epitaxial film of $PbSr_2CuO_{5+\delta}$ by molecular beam epitaxy.[7] However, they also reported that the method does not work well for the growth of $PbSr_2CaCu_2O_{7+\delta}$ (Pb1212), because the growth temperature is limited due to the volatility of Pb.[8] Although we attempted to grow PbBi1212 by conventional in-situ sputtering, we never obtained single-phase films of PbBi1212 because of the re-evaporation of Pb and Bi from the substrate.

In the present paper, we describe a two-step growth technique[9] that allows us to maintain the chemical composition of the film: PbBi1212 deposited on a $SrTiO_3$ (STO) substrate at low temperature forms an amorphous film which at high temperature, crystallizes with the crystallographic symmetry of the substrate. We demonstrated that this technique works well for fabricating the single-phase PbBi1212 epitaxial films. It is found that the PbBi1212 system exhibits superconductivity at approximately 50 K. We also clarify various superconducting properties of Pb1212 system such as substitution effects, coherence lengths, and anisotropy. The two-step growth technique may provide a method to fabricate next generation superconducting wires from ubiquitous elements.

II. CRYSTAL GROWTH AND EXPERIMENTAL METHODS

PbBi1212 epitaxial film was grown by a two-step technique consisting of a low temperature sputtering step and a high temperature ex-situ growth step. Sputtering targets were synthesized by the solid state reaction method using high purity powders (> 99.9 %) of PbO, Bi_2O_3, $SrCO_3$, Y_2O_3, $CaCO_3$, and CuO. These powders were mixed into compositions of $(Pb_{0.75}Bi_{0.25})_{1.5}Sr_2Y_{1-x}Ca_xCu_{2.6}O_z$ ($x = 0.4 - 0.7$) and calcined two times: first at 860 °C for 10 h in air and then at 880 °C for 10 h in air. After calcination, the powders were pressed into cylindrical pellets 100 mm in diameter and 7 mm in height, and they were sintered at 1020 – $200x$ °C for 24 h in air, where x is the Ca concentration. For depositing the PbBi1212 amorphous films on STO (100) substrates, we used the following sputtering conditions: the sputtering gas pressure was 100 mTorr (60 sccm Ar and 15 sccm O_2), the anode voltage was 1.4 kV, and the substrate temperature was

approximately 200 °C (the substrates were not heated). The deposition time was set to 1 – 2 h. The thickness of the PbBi1212 thin films measured by a stylus-based profilometer was 1800 – 3500 Å.

PbBi1212 containers used for ex-situ growth were made of polycrystalline pellets prepared in the same way as the sputtering targets at compositions of $Pb_{1-y}Bi_ySr_2Y_{0.3}Ca_{0.7}Cu_2O_z$ ($y = 0$ – 0.5). The mixed powders were calcined three times at 880 °C for 10 h in air, pressed into two cylindrical pellets 26 mm in diameter and 5 mm in height, and sintered at 1007 °C for 3 h in air. For epitaxial growth, amorphous films on STO substrates were placed in a pit ($8 \times 8 \times 2$ mm^3) formed at the center of one of the sintered pellets. The other pellet was used as a lid for the growth container. The container containing the amorphous film was heated in a muffle furnace at 970 °C for 6 h under an O_2 atmosphere and cooled to room temperature at a rate of 200 °C/h. The concentration of Pb and Bi in the films was determined by energy dispersive X-ray spectroscopy (EDS), and it was found to change drastically during the film growth. The concentration of Pb and Bi is dominated by the composition of the growth container, whereas the concentrations of the other elements in the films are dominated by the composition of the sputtering target.

As-grown films are not superconducting and a subsequent quenching treatment is necessary to make them superconducting. In this treatment, the film was placed in a quartz tube and heated at 815 °C in air for 1 h. Within two seconds after removing the quartz tube from the furnace, it was placed in liquid nitrogen. This procedure makes the film superconducting, as for the case of bulk polycrystalline PbCu1212, as reported by Maeda et al.[5] This quenching process reduces the c-axis lattice constant (approximately 0.03 Å), which increases the hole concentration. We attribute these changes to a decrease in oxygen content and a change in the valence of Pb ions from 2+ to 4+. The Hall coefficient and temperature dependence of the resistivity under magnetic field were measured by the ac four probe method with a physical properties measurement system (Quantum Design Co. Ltd.). The Hall coefficient was determined at various temperatures by a linear fit to the transverse resistivity as a function of external magnetic field ($B \parallel c$) between ± 5 T.

III. RESULTS AND DISCUSSION

A. Crystallographic characterization

Figure 1(a) shows the out-of-plane X-ray diffraction (XRD) θ–2θ scan results for a thin film of a single-phase PbBi1212. This data indicates the complete c-axis alignment of the film. In thin films of single-phase PbBi1212, the peaks from other phases were completely absent or less than 0.5 % of the peak magnitude for PbBi1212 (005). It was found a Ca concentration of $x < 0.36$ and a Bi concentration of $y < 0.20$ are required to obtain single-phase PbBi1212 films. Impurity phases such as Bi2212

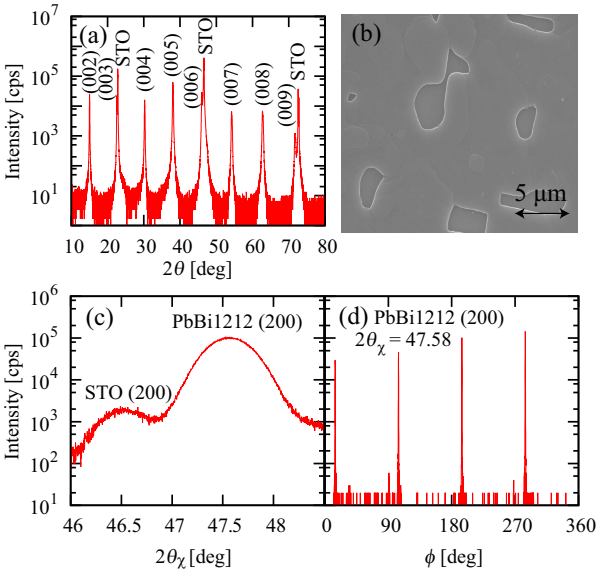

FIG. 1: For single-phase PbBi1212 thin film: (a) out-of-plane XRD θ–2θ scan, (b) surface morphology, (c) in-plane XRD $2\theta_\chi$–ϕ scan pattern around (200) peaks of PbBi1212 and STO, and (d) ϕ scan pattern at PbBi1212 (200) ($2\theta_\chi = 47.58°$).

were detected in samples whose concentrations of Ca or Bi exceeded these limits. To prevent the growth of the impurity phase, the Ca concentration of the sputtering target has to be less than 0.5 and the Bi concentration of the growth container has to be less than 0.25. The c-axis lattice constant of the sample in Fig. 1(a) is 11.846 Å , which is shorter than the c-axis lattice constant of the bulk sample ($c = 11.866$ Å[10]) with nearly the same composition.

Figure 1(b) shows an image of the surface of a thin film of single-phase PbBi1212. The image was acquired by scanning electron microscopy. The surface morphology of the film is smooth except for a few steps. This morphology implies that film growth progresses along the surface of the substrate. Note that no cracks, grain boundaries, and impurity phase precipitations were found on the entire surface of the film.

We used in-plane XRD measurements to check whether the films grow epitaxially on the substrates. Figure 1(c) shows the result of a $2\theta_\chi$–ϕ scan for a single-phase PbBi1212 film. The peaks of STO (200) and PbBi1212 (200) are identified. This result shows that lattice relaxation occurs from the 2 % in-plane lattice mismatch between STO ($a = 3.905$ Å) and PbBi1212 ($a = 3.81$–3.83 Å). The result of an in-plane ϕ scan at the peak of PbBi1212 (200) ($2\theta_\chi = 47.58°$) is displayed in Fig. 1(d). Four peaks are found at 90° between each peak, and the difference in the angle of the peak between STO and PbBi1212 is less than 0.7°. These results indicate that the PbBi1212 thin films grow epitaxially on STO (100) substrates and that tensile strain is exerted from the STO substrates along the a-axis of PbBi1212. This result explain the smaller c-axis lattice constant of PbBi1212 thin film compared with that of a bulk sample.

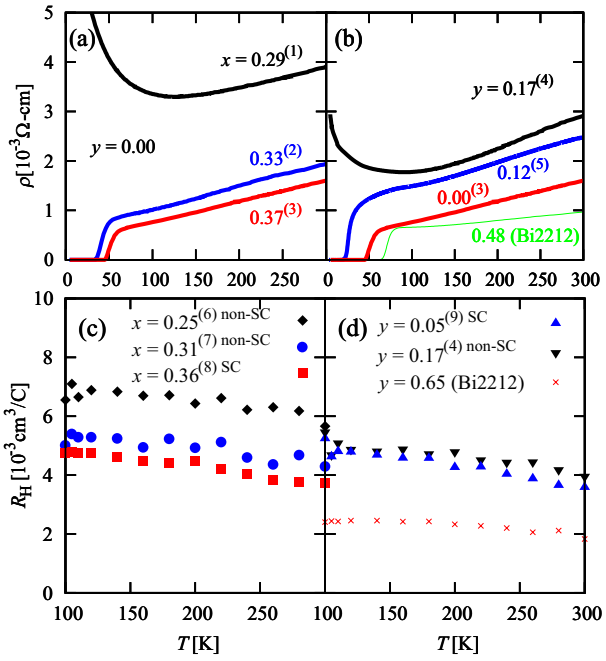

FIG. 2: Temperature dependence of resistivity and Hall coefficients for samples with different Ca and Bi concentrations. (a) The black, blue, and red curves represent data for (x, y) = (0.29, 0.00), (0.33, 0.00), and (0.37, 0.00). (b) The black, blue, red, and green curves represent data for (x, y) = (0.35, 0.17), (0.35, 0.12),(0.37, 0.00), and (0.49, 0.48). (c) The black diamonds, blue circles, and red squares represent data for (x, y) = (0.25, 0.15), (0.31, 0.13), and (0.36, 0.17). (d) The black triangles, blue triangles, and red crosses represent data for (x, y) = (0.35, 0.05), (0.35, 0.17), and (0.50, 0.65). The numbers in parentheses correspond to those in Fig. 3.

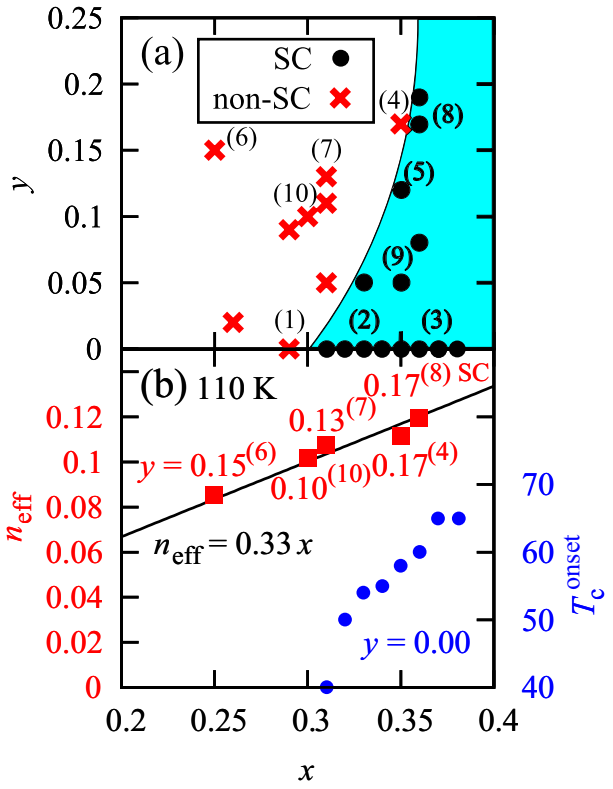

FIG. 3: (a) Distribution of Ca and Bi concentrations in single-phase samples and the superconductivity of these samples. The black circles correspond to the superconducting samples and the red crosses correspond to the non-superconducting samples. The hatched area shows the range of concentration for which superconducting films are obtained. (b) Effective hole density $n_{\rm eff}$ (red squares, left axis) for various Bi concentrations y and $T_{\rm c}^{\rm onset}$ (black circles, right axis) for $y = 0$ as a function of Ca concentration x.

B. Substitution effect

Figures 2(a) and 2(b) show the temperature dependence of the resistivity for samples with different Ca and Bi concentrations, respectively. The composition of the film was determined by EDS at three different points (25×25 μm^2 for each point). As shown in Fig. 2(a), an increase in Ca concentration x leads to a decrease in resistivity and $x > 0.3$ is necessary for the superconducting transition. Notably, a very small increase in Ca concentration induces a transition from an insulator to a superconductor. However, further increasing the Ca concentration does not significantly affect $T_{\rm c}$. In contrast, replacing Pb with Bi up to $y = 0.17$ drastically decreases $T_{\rm c}$, as shown in Fig. 2(b). For $y > 0.20$, the films include $Bi_2Sr_2CaCu_2O_{8+\delta}$ (Bi2212) as a secondary phase and exhibit distinctly different properties than the single-phase films. The resistivity decreases with increasing Bi concentration and even without the quenching treatment, a sharp superconducting transition takes place at 80 K. Also, the XRD peaks of the Bi2212 phase become more intense. Therefore, we conclude that the superconducting transition observed for $y > 0.20$ is due to the Bi2212 impurity phase.

The temperature dependence of the Hall coefficient for different Ca and Bi concentrations is shown in Figs. 2(c) and (d). Figure 2(c) suggests that replacing of Y by Ca increases the hole concentration. However, as shown in Fig. 2(d), no significant change in the Hall coefficient as a function of Bi concentration is observed for the single-phase samples ($y < 0.20$). The significant decrease of Hall coefficient for $y > 0.20$ is attributed to the Bi2212 impurity phase. We find that the slight increase in hole concentration from $x = 0.31$ to 0.36 causes superconductivity in the case of $y \approx 0.15$. All non-superconducting samples are insulators at low temperatures. This sudden change from insulator to superconductor is quite particular to this PbBi1212 system. In contrast, Bi substitution does not introduce holes, but it introduces lattice disorder that strongly decreases $T_{\rm c}$, especially at $x \approx 0.32$. This is consistent with the $\rho(T)$ the data in Figs. 2(a) and 2(b), where the residual resistivity [determined by the linear extrapolation of $\rho(T)$ data above $T_{\rm c}$ crosses $T = 0$] increases with y.

The substitution effect found in this study is sum-

marized in Fig. 3(a). This plot clearly illustrates that, for superconductivity in PbBi1212, a Ca concentration $x > 0.3$ is essential and a lower Bi concentration is preferable. The effective number of holes per Cu atom ($n_{\rm eff} = V_{\rm Cu}/R_{\rm H}e$) as a function of Ca concentration x for various Bi concentrations y is plotted in Fig. 3(b), where $V_{\rm Cu}$ is the unit cell volume for a Cu atom. The quantity $n_{\rm eff}$ depends linearly on x, irrespective of y. For $y = 0.17$, the superconductivity occurs at $n_{\rm eff} = 0.12$, which is between the hole number for optimum $YBa_2Cu_3O_{7-\delta}$ (YBCO) ($T_{\rm c} = 90$ K, $n_{\rm eff} = 0.28$) and the hole number for the superconductor-insulator transition ($n_{\rm eff} = 0.027$).[11] This trend is the same as for $La_{2-x}Sr_xCuO_4$ (LSCO).[12] Therefore, we expect a further increase in $T_{\rm c}$ for our sample upon doping with more hole carriers. In fact, we find that for samples with $y = 0$, $T_{\rm c}^{\rm onset}$ increases with x up to $x = 0.36$, as shown in Fig. 3(b). The linear fit shown in Fig. 3(b) suggests that carrier doping is governed by the substitution of Y^{3+} for Ca^{2+} and 0.33 holes are introduced by the substitution of a Ca^{2+} ion. This is similar to the underdoped region in LSCO[13] and YBCO[11], where the effective number of holes is well described as $n_{\rm eff} \propto x$. The remarkable point of doping in Pb1212 is that fitting line is extrapolated to the zero point of $n_{\rm eff}$. This indicates that all the transport carriers are originated from the Ca substitution, and all the doped carriers contribute as the transport carriers. Therefore, unlike YBCO and LSCO, no doped carriers are localized or used for the formation of the spin (charge) stripes.

As x is increased above 0.37, $T_{\rm c}$ remains constant, whereas at 300 K, ρ decreases. This implies that increasing x creates not only hole carriers but also lattice deformation that is more sensitive to the emergence of the superconductivity than to the normal-state conductivity. The (Y, Ca) site of Pb1212 is inside the CuO_2 double layer, as is the case for (Y, Ca)$Ba_2Cu_3O_7$ with $T_{\rm c}$ approximately equal to 90 K. Eisaki et al. pointed out the strong influence of the (Y, Ca) site disorder on $T_{\rm c}$.[14] Concerning Ca substitution at $y = 0$, we conclude that chemical disorder prevents the increase in $T_{\rm c}$ expected from hole doping. To obtain the highest $T_{\rm c}$ for this material, the film properties must be further optimized.

C. Superconducting anisotropy

Figures 4(a) and 4(b) show that the temperature dependence of resistivity for a single-crystal film ($y = 0.00$) in a magnetic field of up to 9 T for $B \parallel c$ and $B \parallel ab$ for the Bi-free ($y = 0.00$) sample. The zero-field transition is significantly broadened by applying $B \parallel c$, whereas the transition is broadened only slightly for $B \parallel ab$. No sharp transition, indicating the vortex lattice melting transition,[15] is observed. This result is attributed to the distribution of superconducting condensation energy accompanied by an inhomogeneous oxygen concentration and lattice disorder in the film.

To discuss the superconducting anisotropy, the upper critical field $B_{\rm c2}$ and the irreversibility field $B_{\rm irr}$ are defined by the criteria of $\rho/\rho_{\rm n} = 90$ % and $\rho = 1 \times 10^{-5}$ Ω-cm, respectively. $B_{\rm c2}$ and $B_{\rm irr}$ for $B \parallel c$ and $B \parallel ab$ are plotted in Fig. 4(c) as a function of temperature. The quantities $B_{\rm c2}^{c}(0)$ and $B_{\rm c2}^{ab}(0)$ are estimated to be 54 and 492 T, respectively, by using the Werthamer-Herfand-Hohenberg (WHH) theory[16], which gives $B_{\rm c2}(0) = -0.69 T_{\rm c} (dB_{\rm c2}/dT)|_{T_{\rm c}}$. By using $B_{\rm c2} = \Phi_0/2\pi\xi^2$, the coherence lengths ξ were derived as $\xi_{ab}(0) = 25$ Å and $\xi_c(0) = 2.7$ Å. Consequently, the anisotropy, $\gamma = \xi_{ab}(0)/\xi_c(0)$ is estimated to be 9.2. This anisotropy is similar to that of bulk Tl1212 ($\gamma \sim 10$)[17] and Hg1212 ($\gamma \sim 7.7$).[18] A further reduction of anisotropy was observed for Bi-doped samples (e.g., $\gamma = 6.5$ with $y = 0.12$), although the $T_{\rm c}$ of these samples are lower than those of Bi-free samples as discussed above. The reduced anisotropy is presumably caused by the decrease in the distance between adjacent CuO_2 double layers because the ionic radius of Bi^{5+} is smaller than that of Pb^{4+}.[19] These results reveal that the anisotropy of PbBi1212 is much less than that of the modulation-free PbBi2212 ($\gamma \sim 25$).[20] This implies that replacing the double (Pb, Bi)O block layers by monolayers results in a reduction in superconducting anisotropy and an enhancement of the coupling between CuO_2 layers.

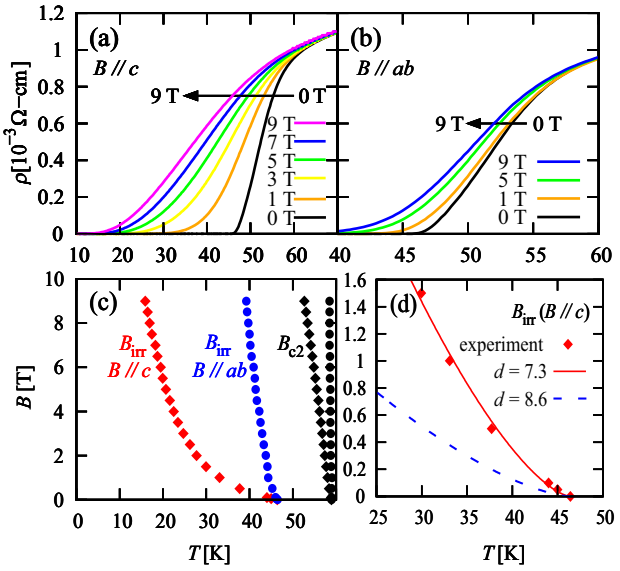

FIG. 4: Temperature dependence of resistivity for (a) $B \parallel c$ and (b) $B \parallel ab$. (c) Irreversibility fields and upper critical fields in sample with (x, y) = (0.31, 0.00). In panel (c), diamond and circle symbols represent data for $B \parallel c$ and $B \parallel ab$, respectively. Solid and broken lines in panel (d) are obtained from the empirical formula with $d = 7.3$ and 8.6, respectively.

Figure 4(d) is an enlarged plot of $B_{\rm irr}$ for $B < 1.6$ T. It also shows the results of fitting the data to the empirical function
$B_{\rm irr}[{\rm T}] = 2\times10^3 \exp(-0.78d)(1-T/T_{\rm c})^{1.5}$ ($T > 0.7\,T_{\rm c}$)[21], where d [Å] is the distance between adjacent CuO_2 planes. The curve fit gives the value of $d = 7.3$ Å, which is less than the result of $d = 8.4$ Å from crystal structure

refinements based on X-ray and neutron diffraction.[10] Based on EDS analysis of the film, a considerable portion of Pb ions in the block layer is possibly substituted by Cu ions. Assuming that the substituted sites, which form CuO_6 octahedral sites, accumulate and form CuO_2 single layers and thereby partly spread the film, the effective value of d may be considerably reduced. In YBCO, the empirical formula applies for $d = 4.15$ Å which is close to the distance between the CuO_2 plane and CuO chain.[21]

IV. SUMMARY

We verified the superconducting properties of PbBi1212 by measuring the transport properties of epitaxial films prepared by the two-step technique. Films of single-phase PbBi1212 were obtained with a Ca concentration of less than 0.36 and a Bi concentration of less than 0.20. We found that a Ca concentration greater than 0.3 and a quenching treatment are essential for making the epitaxial films superconducting. Increasing the Ca concentration leads to an increase in the hole density, and increasing the Bi concentration leads to a decrease in the critical temperature T_c. The highest $T_c^{\rm onset}$ found for single-phase PbBi1212 films is 65 K, and for the multiphase film, the drop in resistivity starting at a higher temperature is attributed to the Bi2212 impurity phase. For Pb1212, the coherence lengths estimated from the upper critical field is 25 and 2.7 Å along the ab-plane and c-axis, respectively.

Acknowledgments

This work was partly supported by the Global COE project "Education and Research on Photonics and Electronics Science and Engineering" at Kyoto University.

* Electronic address: komori@sk.kuee.kyoto-u.ac.jp

[1] A. Bauer, P. Zoller, J. Glaser, A. Ehmann, W. Wischert, and S. Kemmler, Physica C **256**, 177 (1996).
[2] H. Frank, R. Stollmann, J. Lethen, R. Müller, L. V. Gasparov, N. D. Zakharov, D. Hesse, and G. Güntherodt, Physica C **100**, 268 (1996).
[3] P. Zoller, A. Ehmann, J. Glaser, W.Wischert, and S. Kemmler-Sack, Physica C **306**, 119 (1998).
[4] D. Schneider, S. Köbel, and L. J. Gauckler, Supercond. Sci. Technol. **13**, 1476 (2000).
[5] T. Maeda, K. Sakuyama, S. Koriyama, H. Yamauchi, and S. Tanaka, Phys. Rev. B **43**, 7866 (1991).
[6] R. A. Hughes, Y. Lu, T. Timusk, and J. S. Prestön, Appl. Phys. Lett. **59**, 2597 (1991).
[7] S. Karimoto and M. Naito, Physica C **338**, 92 (2000).
[8] M. Naito, S. Karimoto, and H. Yamamoto, Proc. SPIE **119**, 4058 (2000).
[9] S. L. Yan, H. L. Cao, X. M. Yang, and X. D. Zhou, J. Appl. Phys. **70**, 526 (1991).
[10] J. Glaser, A. Ehmann, B. Seling, S. Lösch, P. Zoller, W. Wischert, S. Kemmler-Sack, J. Linhart, and W. Reimers, Physica C **276**, 91 (1997).
[11] K. Semba and A. Matsuda, Phys. Rev. Lett. **496**, 86 (2001).
[12] Y. Ando, Y. Kurita, S. Komiya, S. Ono, and K. Segawa, Phys. Rev. Lett. **92**, 197001 (2004).
[13] H. Takagi, T. Ido, S. Ishibashi, M. Uota, S. Uchida, and Y. Tokura, Phys. Rev. B **40**, 2254 (1989).
[14] H. Eisaki, N. Kaneko, D. L. Feng, A. Damascelli, P. K. Mang, K. M. Shen, Z.-X. Shen, and M. Greven, Phys. Rev. B **69**, 064512 (2004).
[15] W. K. Kwok, U. Welp, V. M. Vinokur, S. Fleshler, J. Downey, and G. W. Crabtree, Phys. Rev. Lett. **67**, 390 (1991).
[16] N. R. Werthamer, E. Helfand, and P. C. Hohemberg, Phys. Rev. **147**, 295 (1966).
[17] F. Warmont, V. Hardy, J. Provost, D. Grebille, and C. Simon, Phys. Rev. B **57**, 7485 (1998).
[18] M. S. Kim, S. I. Lee, S. C. Yu, and N. H. Hur, Phys. Rev. B **53**, 9460 (1996).
[19] A. Ehmann, S. Kemmler-Sack, S. Lösch, M. Schlichenmaier, W. Wischert, P. Zoller, T. Nissel, and R. P. Huebener, Physica C **198**, 1 (1992).
[20] R. Gladyshevskii, N. Musolino, and R. Flükiger, Phys. Rev. B **70**, 184522 (2004).
[21] J. Shimoyama, K. Kitazawa, K. Shimizu, S. Ueda, S. Horii, N. Chikumoto, and K. Kishio, Phys. Rev. B **131**, 1043 (2003).